Diffraction at CDF and cross sections at the LHC

K. Goulianos

…some recent references

Presented @ 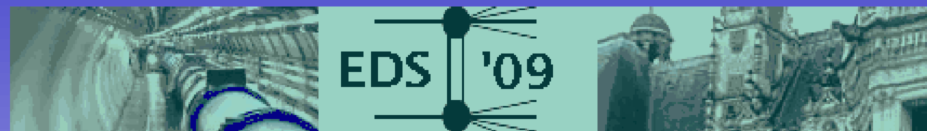

CERN, 29th June - 3rd July 2009

- **Factorization Breaking in Diffraction**
  http://physics.rockefeller.edu/dino/myhtml/talks/goulianos_konstantin_eds09_factorization.pdf
- **The Forward Detectors of CDF and D0**
  …goulianos_konstantin_eds09_detectors.pdf
- **Diffractive and Total pp Cross Sections at LHC**
  …goulianos_konstantin_eds09_sigma.pdf
- **What can we Learn / Expect on Elastic and Diffractive Scattering from the LHC Experiments?** (discussion session – see K. Eggert's talk)
  … goulianos_konstantin_eds09_ discussion.pdf

Contents

1

1 Introduction

2 Diffraction at CDF: 17 PRLs / PRDs

see http://physics.rockefeller.edu/publications.html

3 Current data analyses

Diffractive dijet SF..	- under internal review
DSF in DPE………………	- final stage of analysis
Diffractive W/Z………	- under internal review
Central gaps………………	– towards internal review

4 Cross sections at the LHC

p-p Interactions

Non-diffractive:

Color-exchange

Incident hadrons acquire color and break apart

↑

CONFINEMENT

Diffractive:

Colorless exchange carrying vacuum quantum numbers

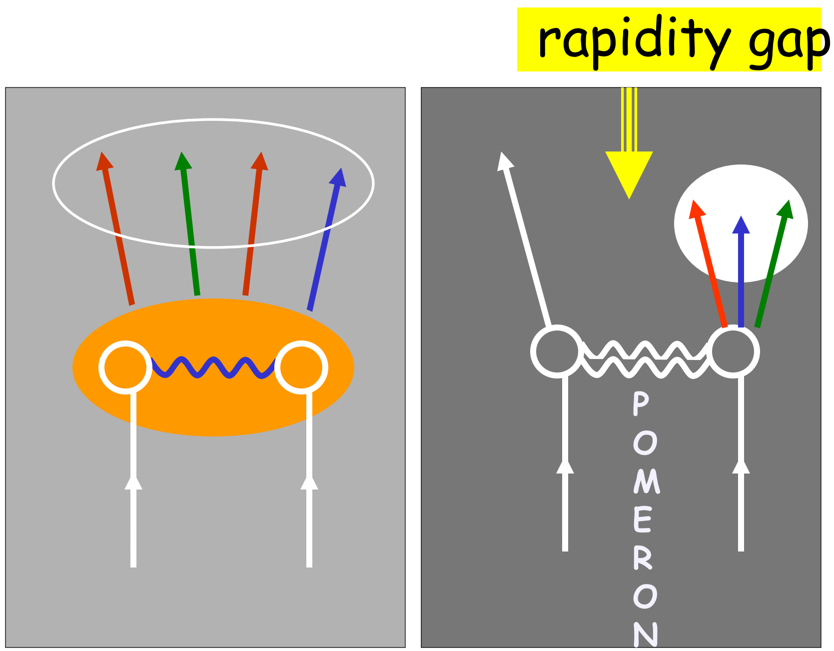

Incident hadrons retain their quantum numbers remaining colorless

↓

pseudo-DECONFINEMENT

Goal: understand the QCD nature of the diffractive exchange

Definitions

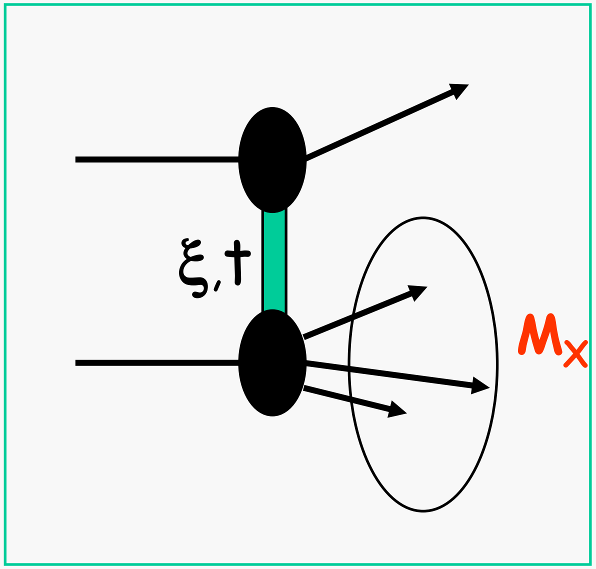

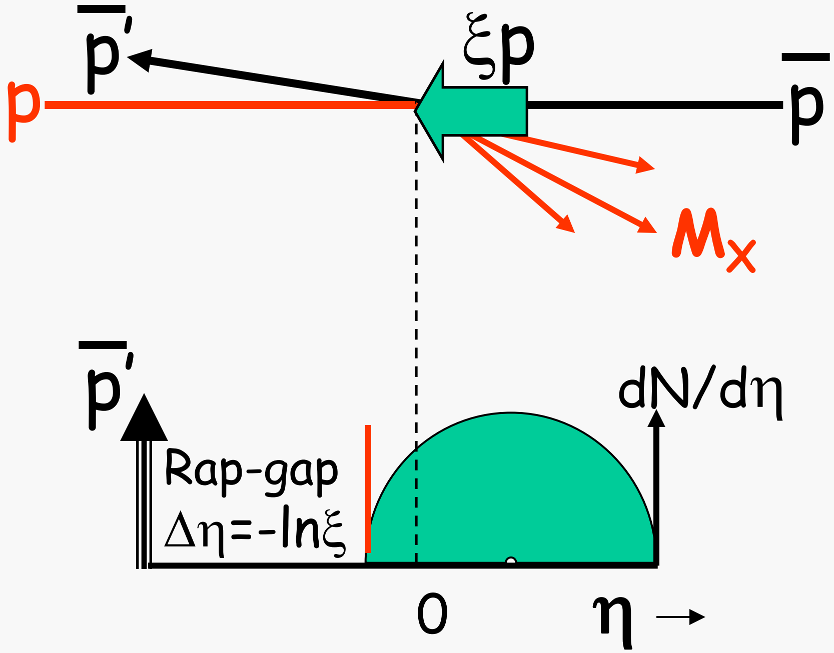

Rapidity Gaps in Fireworks

2

1 Introduction

2 Diffraction at CDF: 17 PRLs / PRDs

see http://physics.rockefeller.edu/publications.html

3 Current data analyses

Diffractive dijet SF..	- under internal review
DSF in DPE………………	- final stage of analysis
Diffractive W/Z………	- under internal review
Central gaps………………	- towards internal review

4 Cross sections at the LHC

Diffraction at CDF

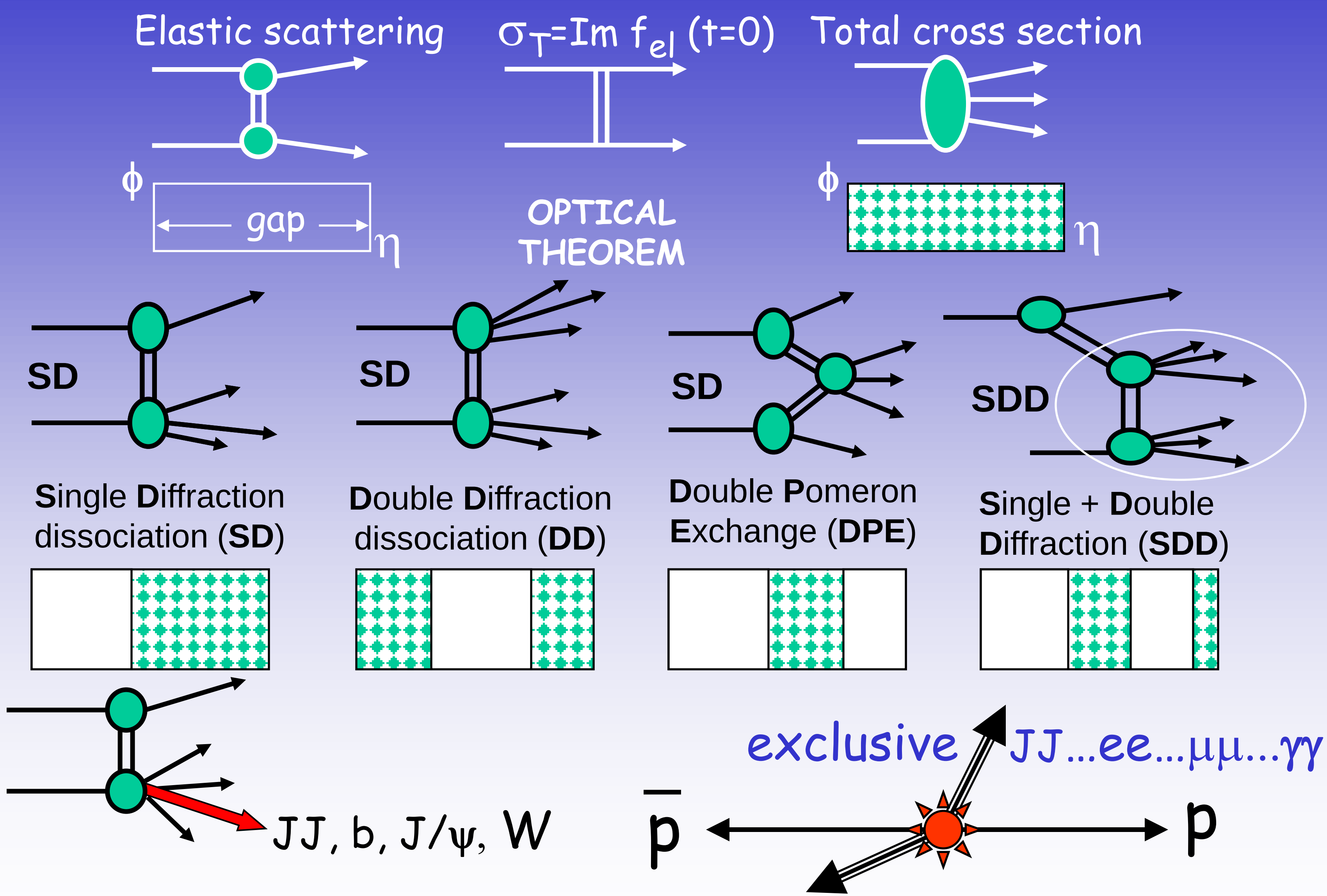

σ^T_{SD} (pp & $\bar{p}p$)

➔ suppressed relative to Regge prediction

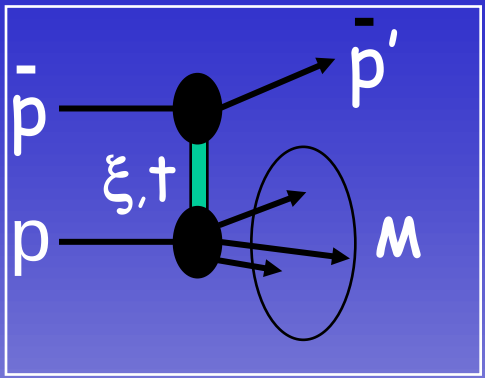

σ^T_{SD} mb

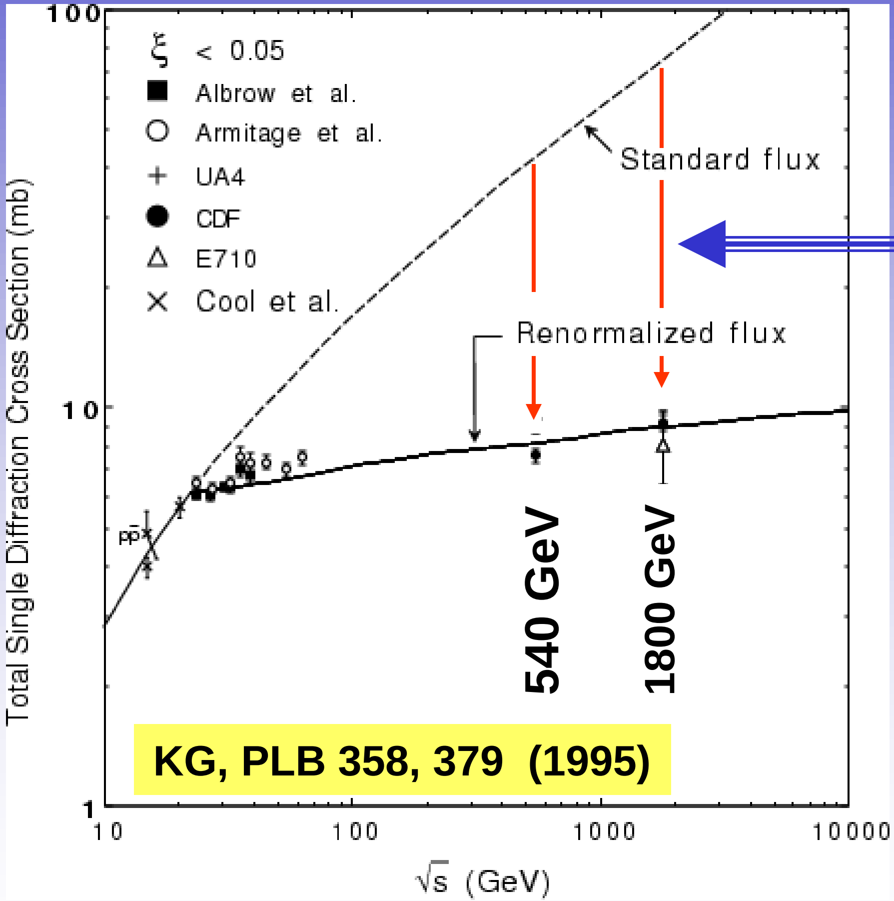

Factor of ~8 (~5) suppression at √s = 1800 (540) GeV

M^2 scaling

➔ ds/dM2 independent of s over 6 orders of magnitude!

renormalization

$$\frac{d\sigma}{dM^2} \propto \frac{s^{2\varepsilon} \rightarrow 1}{(M^2)^{1+\varepsilon}}$$

➔ Independent of s over 6 orders of magnitude in M^2!

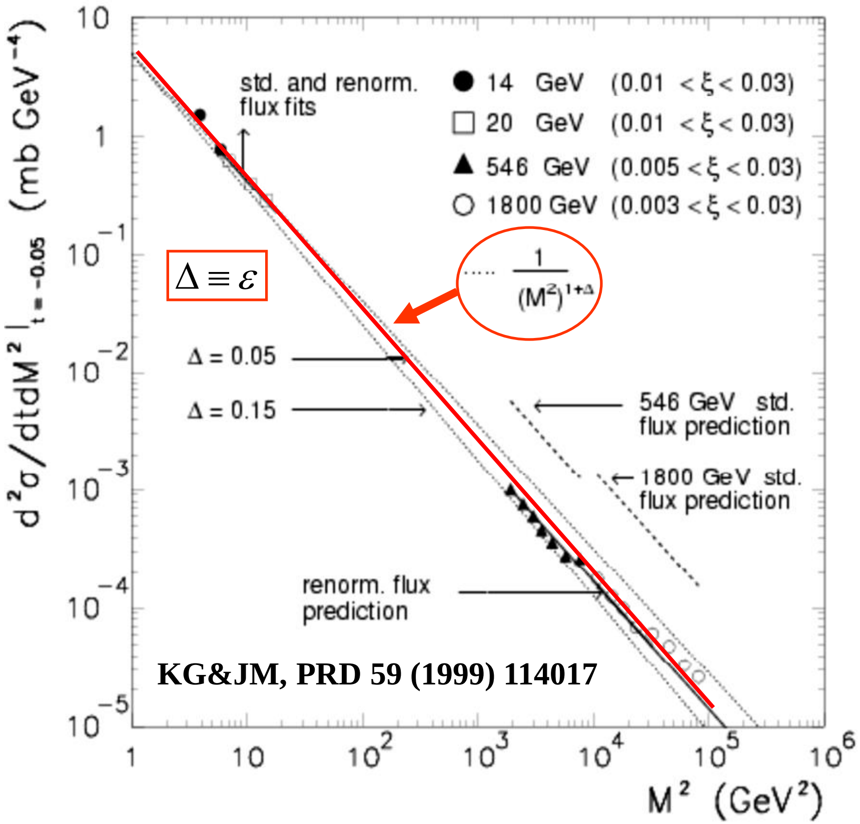

➔ factorization breaks down to ensure M^2 scaling!

Saturation / Single Diffraction

Pomeron flux

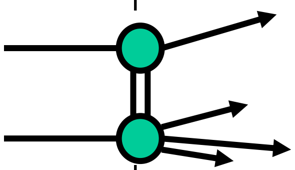

$$\frac{d^2\sigma_{SD}}{dt\,d\xi} = f_{IP/p}(t,\xi)\cdot\sigma_{IP-\bar{p}}(s\xi)$$

s_0^{ε}

$s_0^{-\varepsilon/2}\cdot g_{PPP}(t)$

$$\int_{\xi_{min}}^{0.1}\int_{t=-\infty}^{0} f_{IP/p}(t,\xi)\,d\xi\,dt \Rightarrow 1$$

$\sigma_{SD} \sim s^{2\varepsilon}$

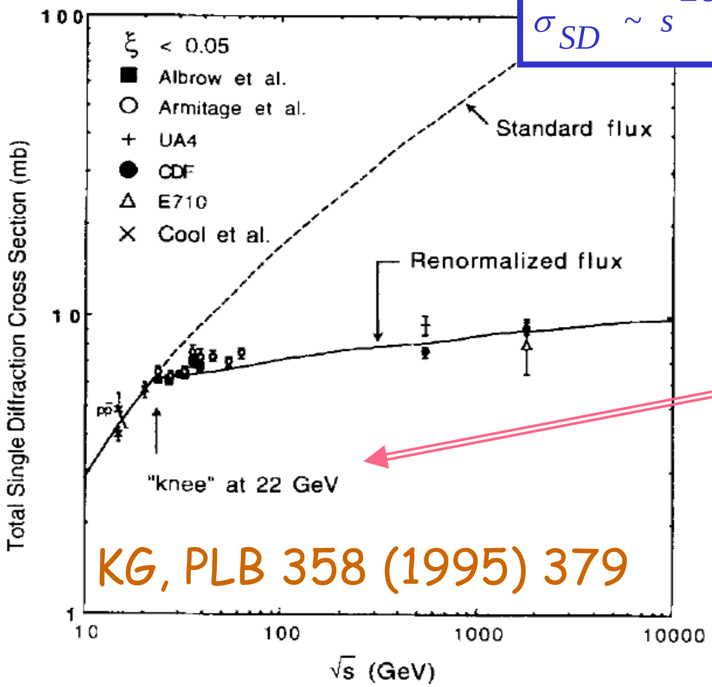

KG, PLB 358 (1995) 379

Renormalization

- $\displaystyle\int_{\xi_{min}\approx 1/s}^{\zeta}\int_{t=-\infty}^{0} f_{IP/p}(t,\xi)\,d\xi\,dt \approx C\cdot s^{2\varepsilon}\cdot s_0^{\varepsilon} \Rightarrow 1$
- Flux integral depends on s and s_0
- "knee" √s-position determines s-value where flux becomes unity ➔ get s_o
- get error in s_o from error in √s-knee

$\delta s_o/s_o = -2\,\delta s/s = -4\,(\delta\sqrt{s})/\sqrt{s}$

Diffractive Structure Function (DSF)

Breakdown of QCD factorization

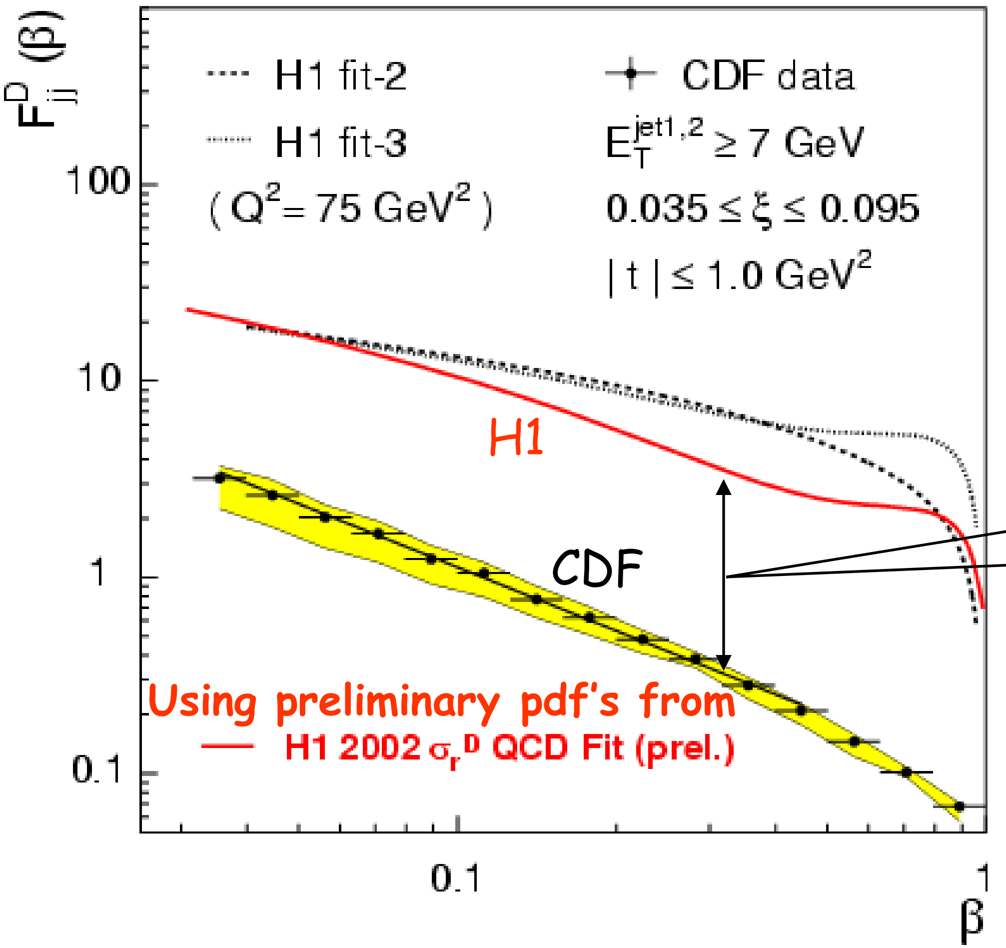

$$\bar{p}p \rightarrow \bar{p} + \text{dijet} + X$$

same suppression
as in soft diffraction

momentum fraction
of parton in Pomeron

σ^{T}_{SD} and dijets

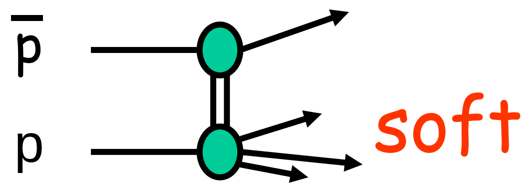

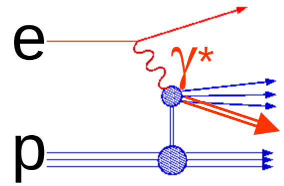

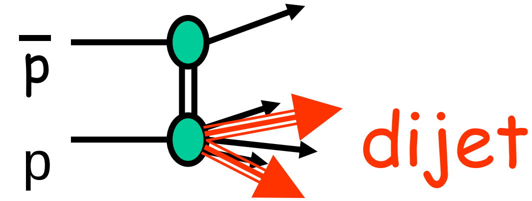

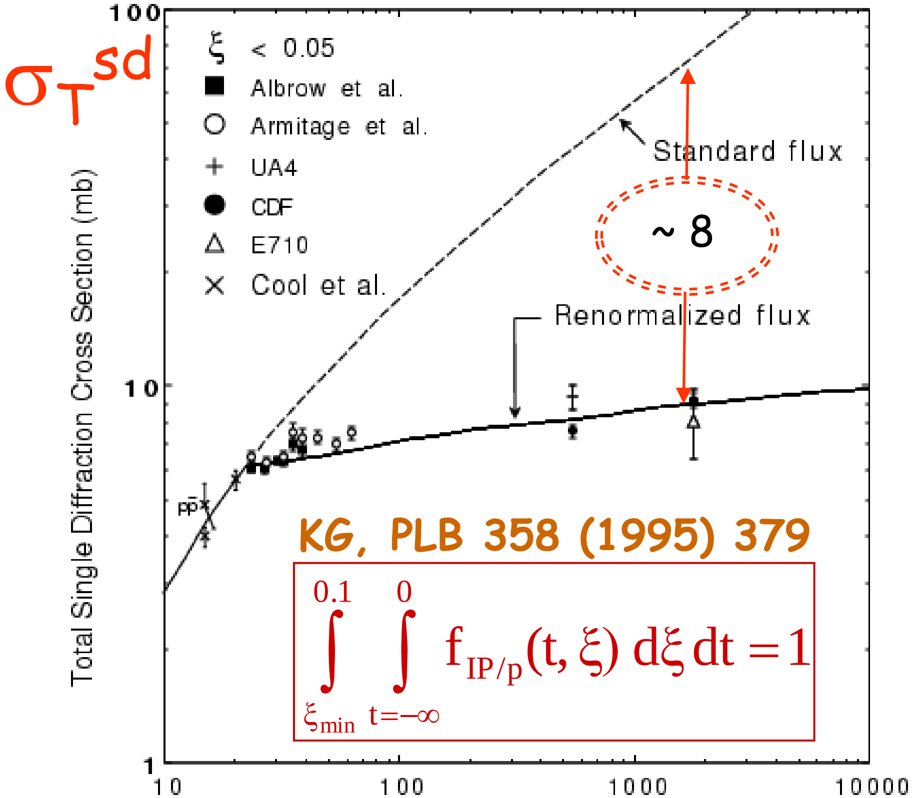

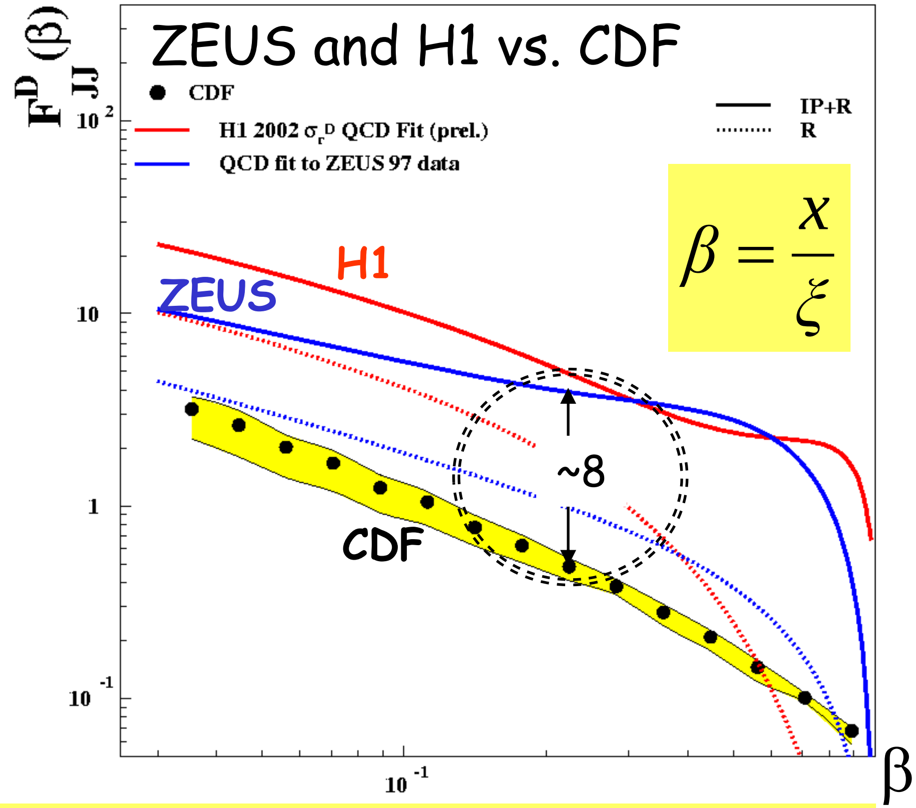

Magnitude: same suppression factor in soft and hard diffraction!
Shape of β distribution: ZEUS, H1, and Tevatron – why different slapes?

Hard diffractive fractions

$$\bar{p}p \rightarrow (\text{✹} + X) + \text{gap}$$

Fraction: SD/ND
@ 1800 GeV

Run I

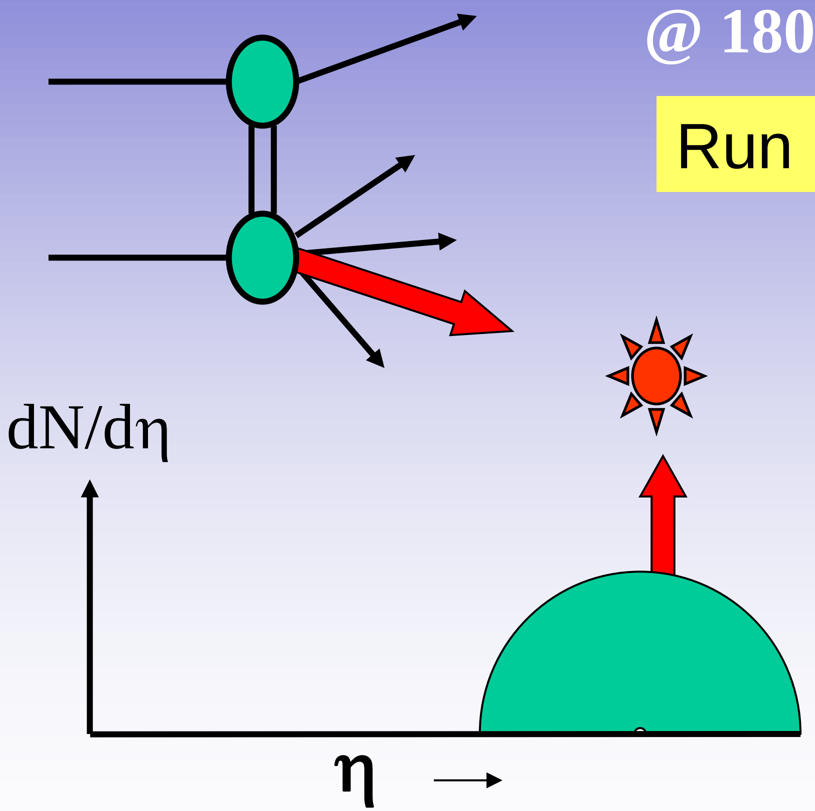

✹	Fraction (%)
JJ	0.75 +/- 0.10
W	0.115 +/- 0.55
b	0.62 +/- 0.25
J/ψ	1.45 +/- 0.25

All fractions ~ 1%
(differences due to kinematics)
- ➢ ~ uniform suppression
- ➢ ~ FACTORIZATION !

Exclusive Dijet and Higgs Production

Phys. Rev. D 77, 052004

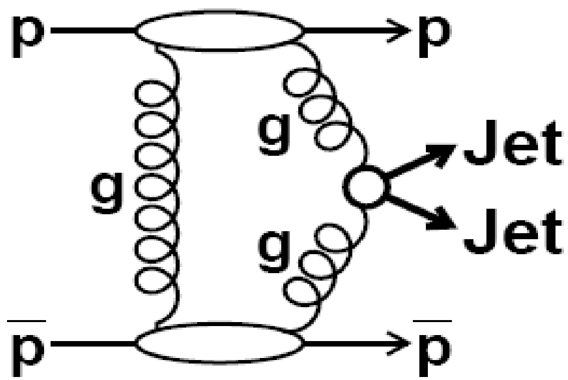

ExHuME

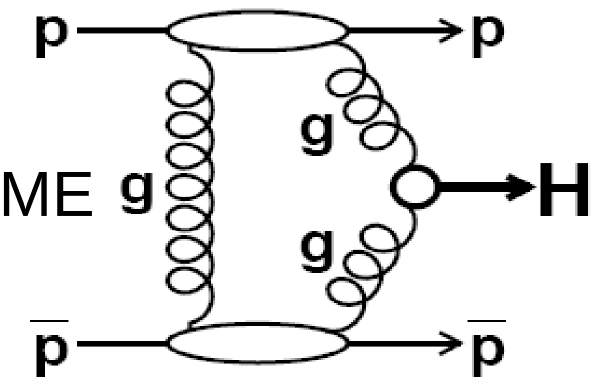

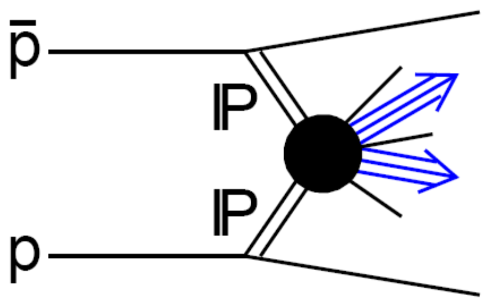

DPEMC

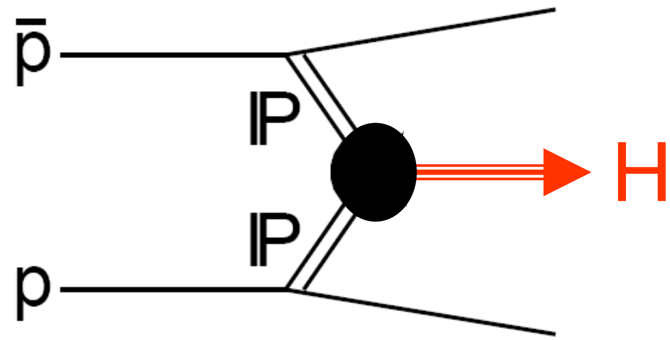

Exclusive Dijet x-section vs. M_{jj}

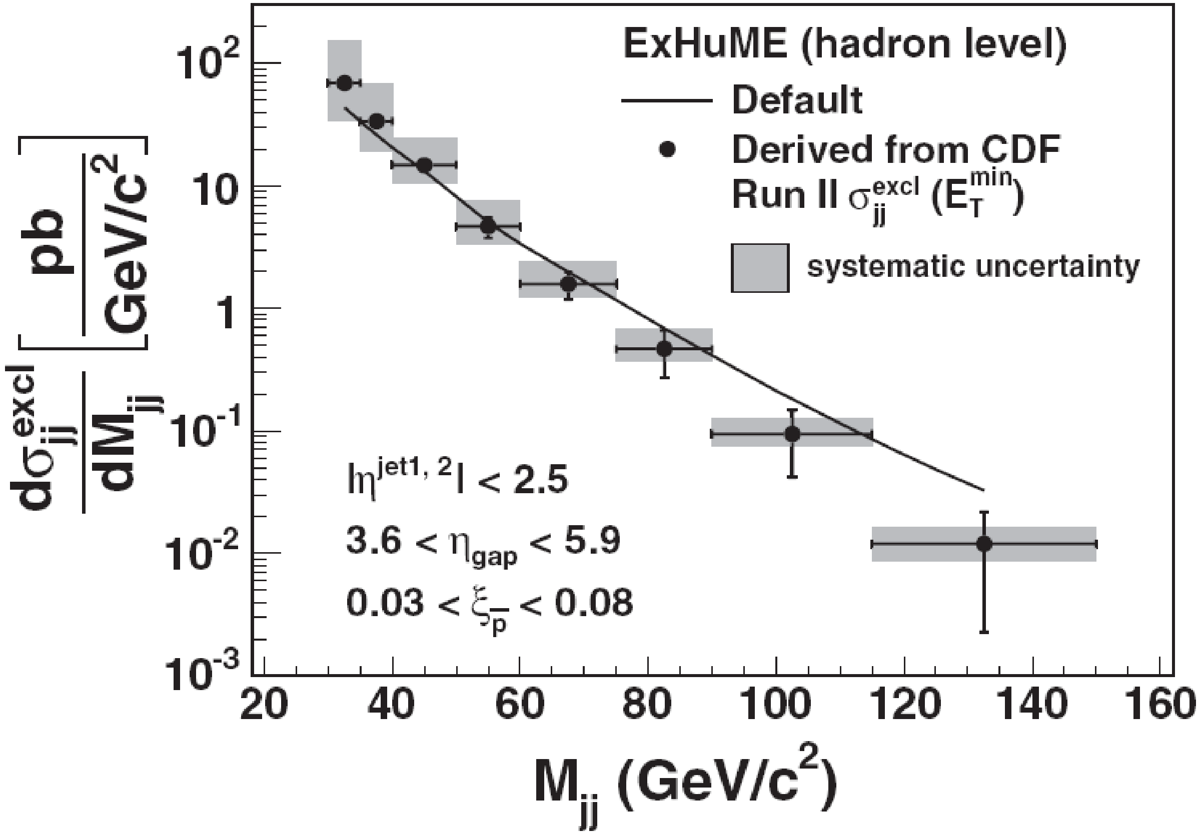

line: ExHuME hadron-level exclusive di-jet cross section vs. di-jet mass

points: derived from CDF excl. di-jet x-sections using ExHuME

Stat. and syst. errors are propagated from measured cross section uncertainties using M_{jj} distribution shapes of ExHuME generated data.

3

1 Introduction

2 Diffraction at CDF: 17 PRLs / PRDs

see http://physics.rockefeller.edu/publications.html

3 Current data analyses

Diffractive dijet SF..	- under internal review
DSF in DPE……………….	- final stage of analysis
Diffractive W/Z……….	- under internal review
Central gaps……………….	– towards internal review

4 Cross sections at the LHC

DSF from Dijets in Run II

$$R(x_{Bj}) \equiv \frac{Rate_{jj}^{SD}(x_{Bj})}{Rate_{jj}^{ND}(x_{Bj})} \Rightarrow \frac{F_{jj}^{SD}(x_{Bj})}{F_{jj}^{ND}(x_{Bj})}$$

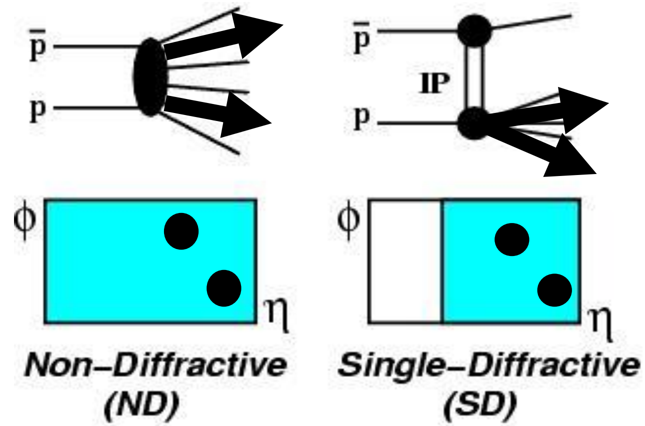

x_{Bj} - distribution

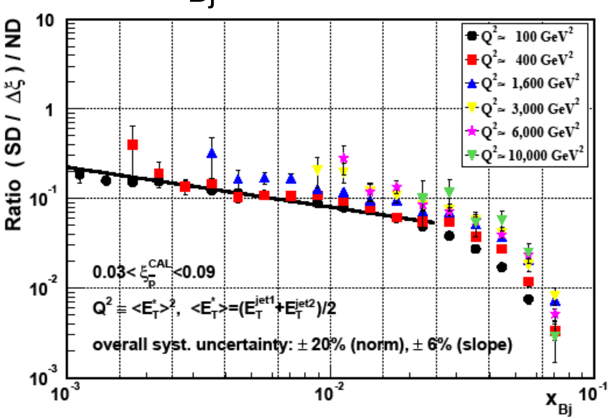

b - slope of t-distribution

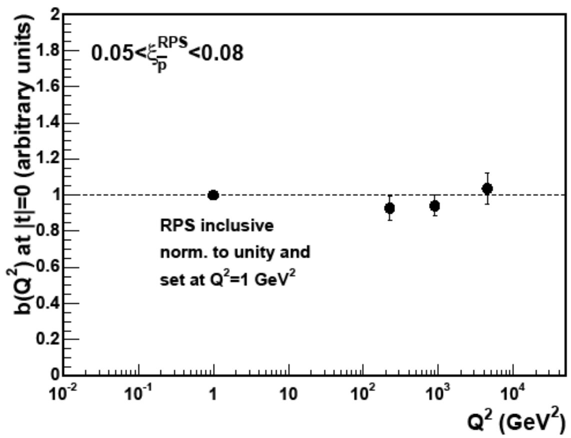

t - distribution

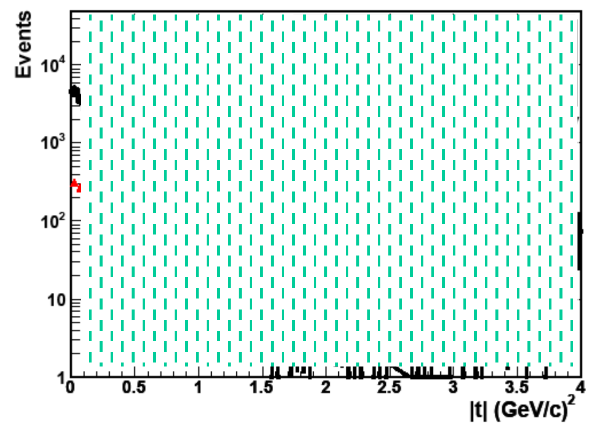

- The x_{Bj}-distribution of the SD/ND ratio has no strong Q^2 dependence
- the slope of the t-distribution is independent of Q^2
- the t-distribution ?????? diffraction minimum ??????

➢ all three results ➔ "first observation"

Dijets - E_T distributions

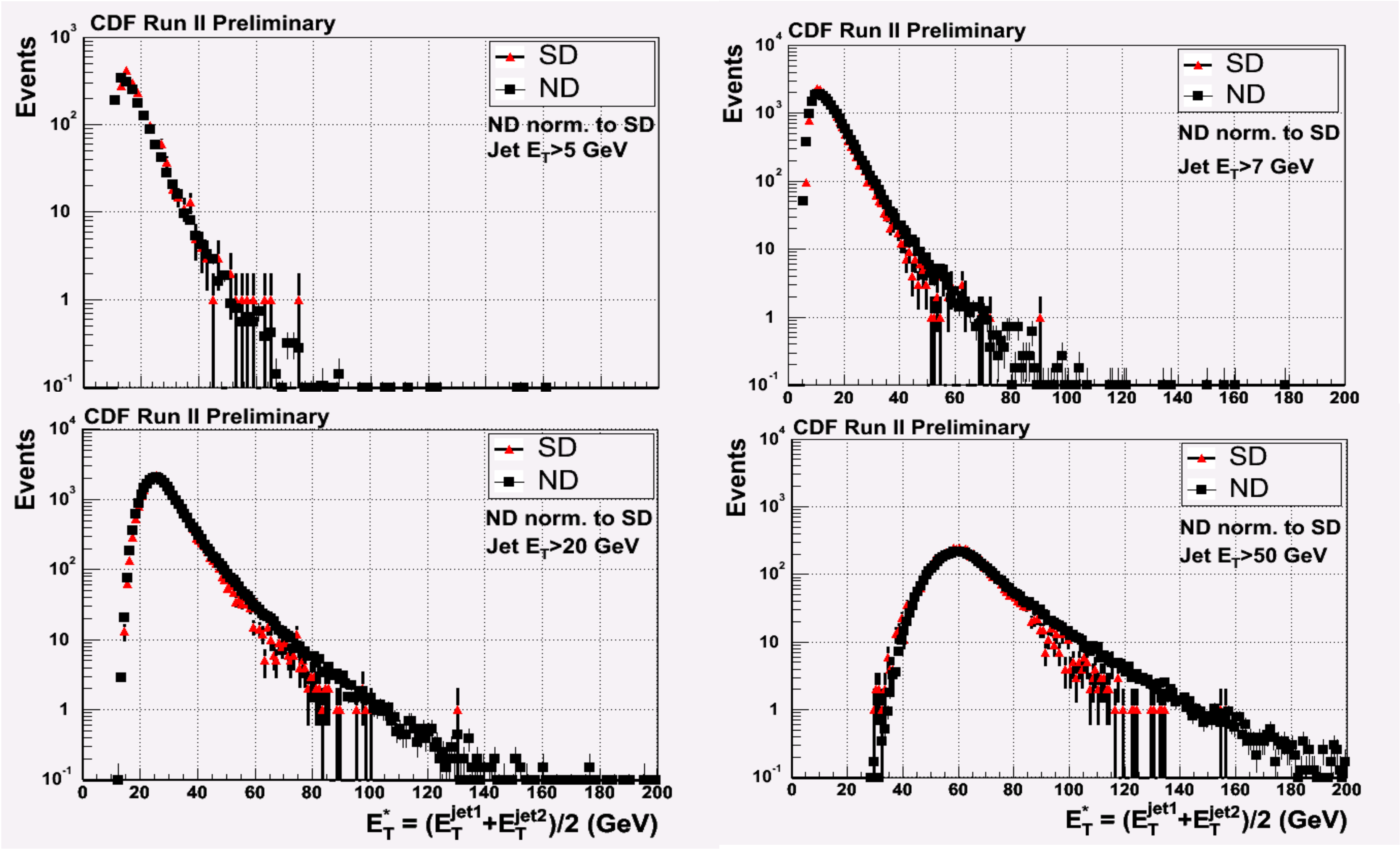

→ similar for SD and ND over 4 orders of magnitude

Kinematics

DSF from Dijets in DPE

Does QCD factorization hold for
the formation of the 2nd gap?

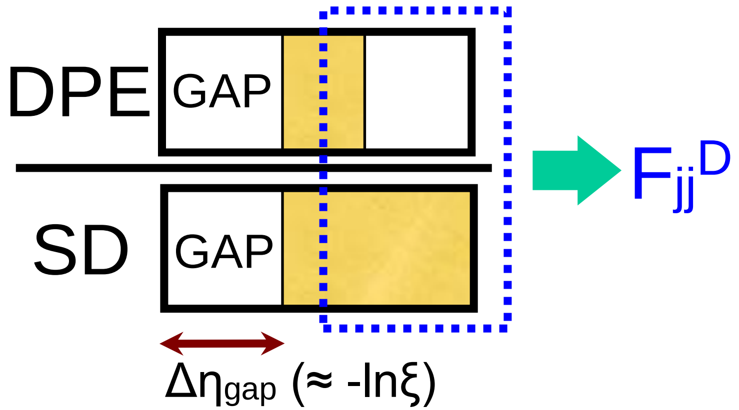

stay tuned…

Diffractive W/Z Production

- probes the quak content of the Pomeron

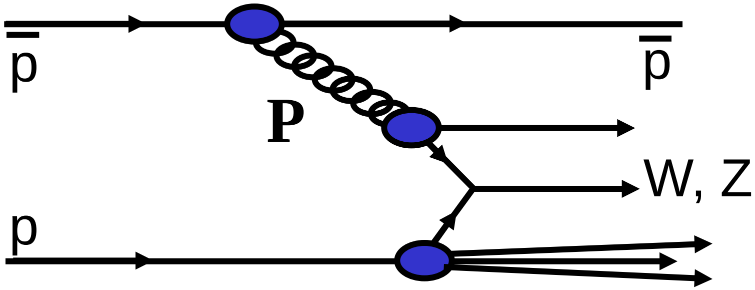

➢ use CAL and Roman pots to get η_ν

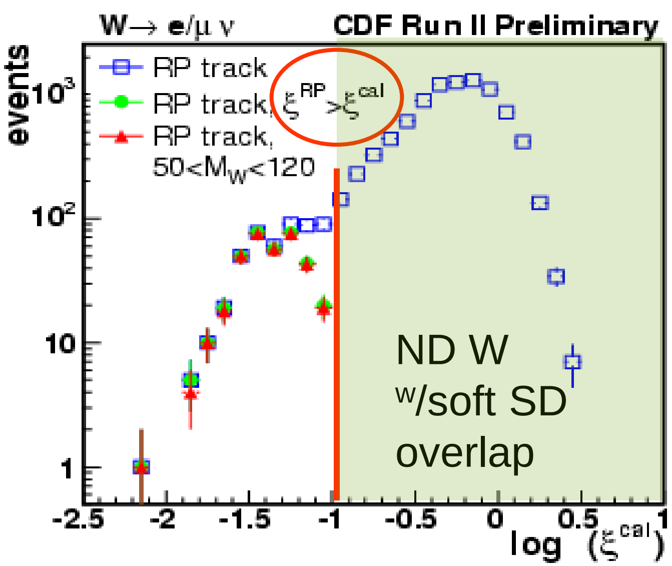

$$\xi^{cal} = \sum_{towers} \frac{E_T}{\sqrt{s}} e^{-\eta}$$

$$\xi^{RPS} - \xi^{cal} = \frac{\not{E}_T}{\sqrt{s}} e^{-\eta_\nu}$$

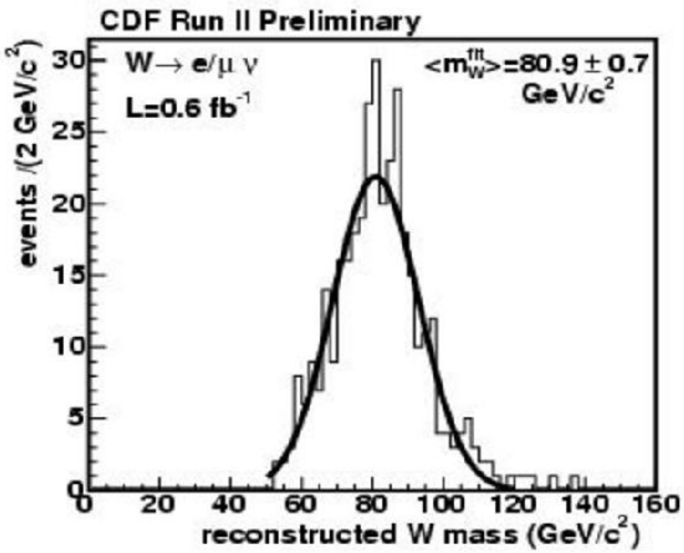

CDF (press release 2007): 80,413 +/- 48 MeV/c^2

RESULTS

R^W ($0.03 < \xi < 0.10$, $|t|<1$)= [0.97 ± 0.05(stat) ± 0.11(syst)]%

Run I: R^W =1.15±0.55 % (ξ<0.1)➔ estimate **0.97±0.47 %** (**$0.03 < \xi < 0.10$ & $|t|<1$**)

R^Z ($0.03 < \xi < 0.10$, $|t|<1$)= [0.85 ± 0.20(stat) ± 0.11(syst)]%

Central gaps

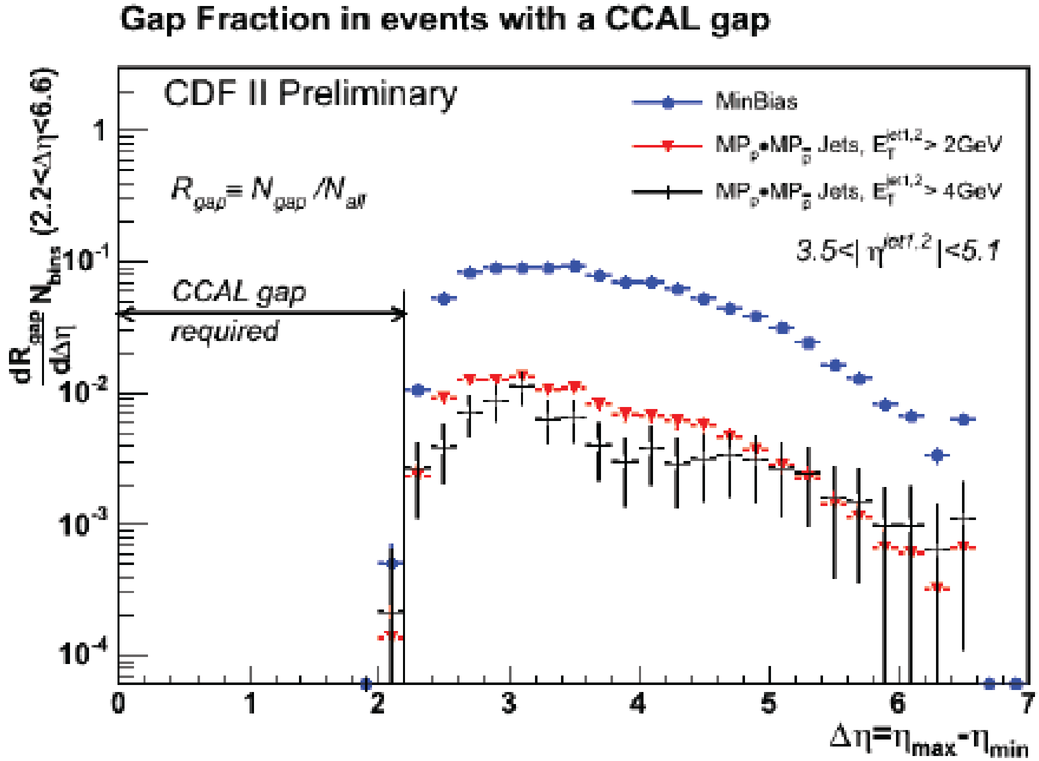

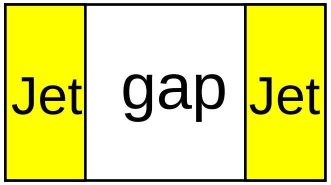

The distribution of the gap fraction $R_{gap}=N_{gap}/N_{all}$ vs $\Delta\eta$ for MinBias ($CLC_p \bullet CLC_{pbar}$) and MiniPlug jet events ($MP_p \bullet MP_{pbar}$) of $E_{T(jet1,2)}>2$ GeV and $E_{T(jet1,2)} > 4$ GeV.

The distributions are similar in shape within the uncertainties.

4

1 Introduction

2 Diffraction at CDF: 17 PRLs / PRDs

see http://physics.rockefeller.edu/publications.html

3 Current data analyses

Diffractive dijet SF..	- under internal review
DSF in DPE....................	- final stage of analysis
Diffractive W/Z..........	- under internal review
Central gaps..................	– towards internal review

4 Cross sections at the LHC

…some references

http://physics.rockefeller.edu/dino/my.html

CDF PRD 50, 5518 (1994) σ^{el} @ 1800 & 546 GeV

CDF PRD 50, 5535 (1994) σ^{D} @ 1800 & 546 GeV

CDF PRD 50, 5550 (1994) σ^{T} @ 1800 & 546 GeV

KG-PR Physics Reports 101, No.3 (1983) 169-219
Diffractive interactions of hadrons at high energies

KG-95 PLB 358, 379 (1995); Erratum: PLB 363, 268 (1995)
Renormalization of hadronic diffraction

CMG-96 PLB 389, 176 (1996)
Global fit to $p^{\pm}p$, $\pi^{\pm}$ and $K^{\pm}p$ cross sections

KG-09 arXiv:0812.4464v2 [hep-ph] 26 March 2009
Pomeron intercept and slope: the QCD connection

Standard Regge Theory

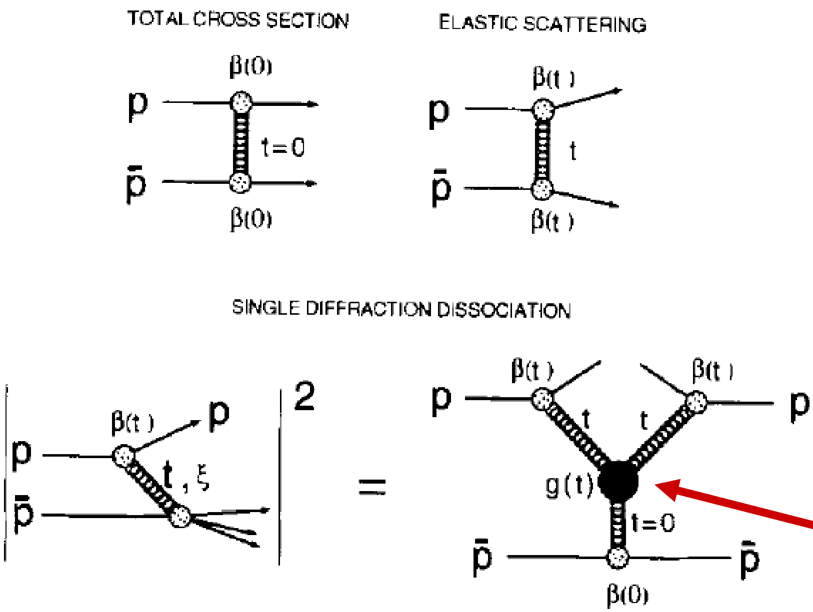

(KG-95)

$$\sigma_T = \beta_1(0)\beta_2(0)\left(\frac{s}{s_0}\right)^{\alpha(0)-1} = \sigma_0^{p\bar{p}}\left(\frac{s}{s_0}\right)^{\epsilon} \quad (1)$$

$$\frac{d\sigma_{el}}{dt} = \frac{\beta_1^2(t)\beta_2^2(t)}{16\pi}\left(\frac{s}{s_0}\right)^{2[\alpha(t)-1]}$$

$$= \frac{\sigma_T^2}{16\pi}\left(\frac{s}{s_0}\right)^{2\alpha' t} F^4(t) \approx \frac{\sigma_T^2}{16\pi} e^{b_{el}(s)t} \quad (2)$$

$$F^4(t) \approx e^{b_{0,el}t} \quad \Rightarrow \quad b_{el}(s) = b_{0,el} + 2\alpha' \ln\left(\frac{s}{s_0}\right) \quad (3)$$

$$\frac{d^2\sigma_{sd}}{dt\,d\xi} = \frac{\beta_1^2(t)}{16\pi}\,\xi^{1-2\alpha(t)}\left[\beta_2(0)\,g(t)\left(\frac{s'}{s'_0}\right)^{\alpha(0)-1}\right]$$

$$= f_{\mathcal{P}/p}(\xi,t)\;\sigma_T^{\mathcal{P}\bar{p}}(s',t) \quad (4)$$

Parameters:

- ❑ s_0, s_0' and g(t)
- ❑ set $s_0' = s_0$ (universal IP)
- ❑ g(t) ➔ g(0) ≡ g_{PPP} see KG-PR
- ❑ determine s_0 and g_{PPP} – how?

Global fit to p±p, π±, K±p x-sections

CMG-96 →

A new determination of the soft pomeron intercept

R.J.M. Covolan[1], J. Montanha[2], K. Goulianos[3]

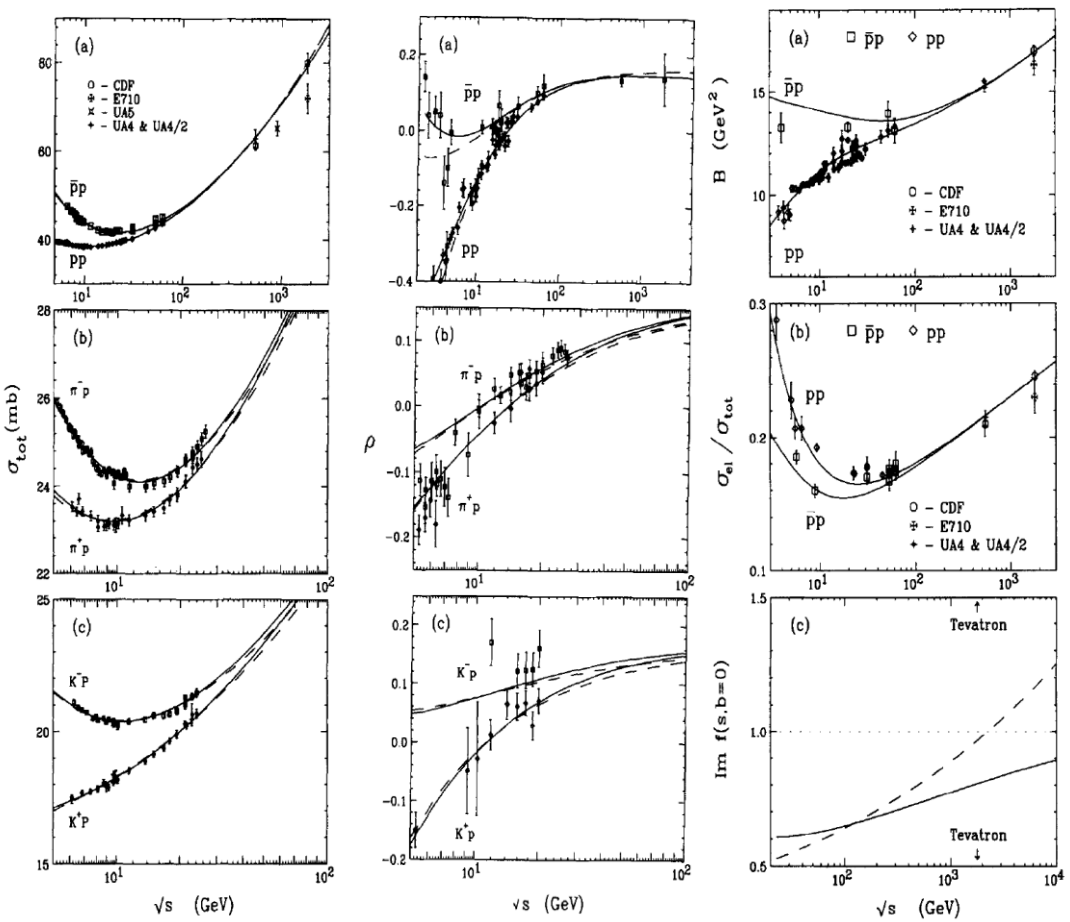

Use standard Regge theory

- INPUT

$$\alpha_{f/a} = 0.68 + 0.82\,t$$

$$\alpha_{\omega/\rho} = 0.46 + 0.92\,t$$

$$\alpha'_{\mathbb{P}} = 0.25\ \text{GeV}^{-2}$$

- RESULTS

$$\alpha_{0,\mathbb{P}}^{\text{Born}} = 1.104 \pm 0.002\,, \quad \alpha_{0,\mathbb{P}}^{\text{Eik}} = 1.122 \pm 0.002$$

$$\sigma_{\text{tot}}^{p^{\pm}p} = 16.79\ s^{0.104} + 60.81\ s^{-0.32} \mp 31.68\ s^{-0.54}$$

negligible

σ^T at LHC from global fit

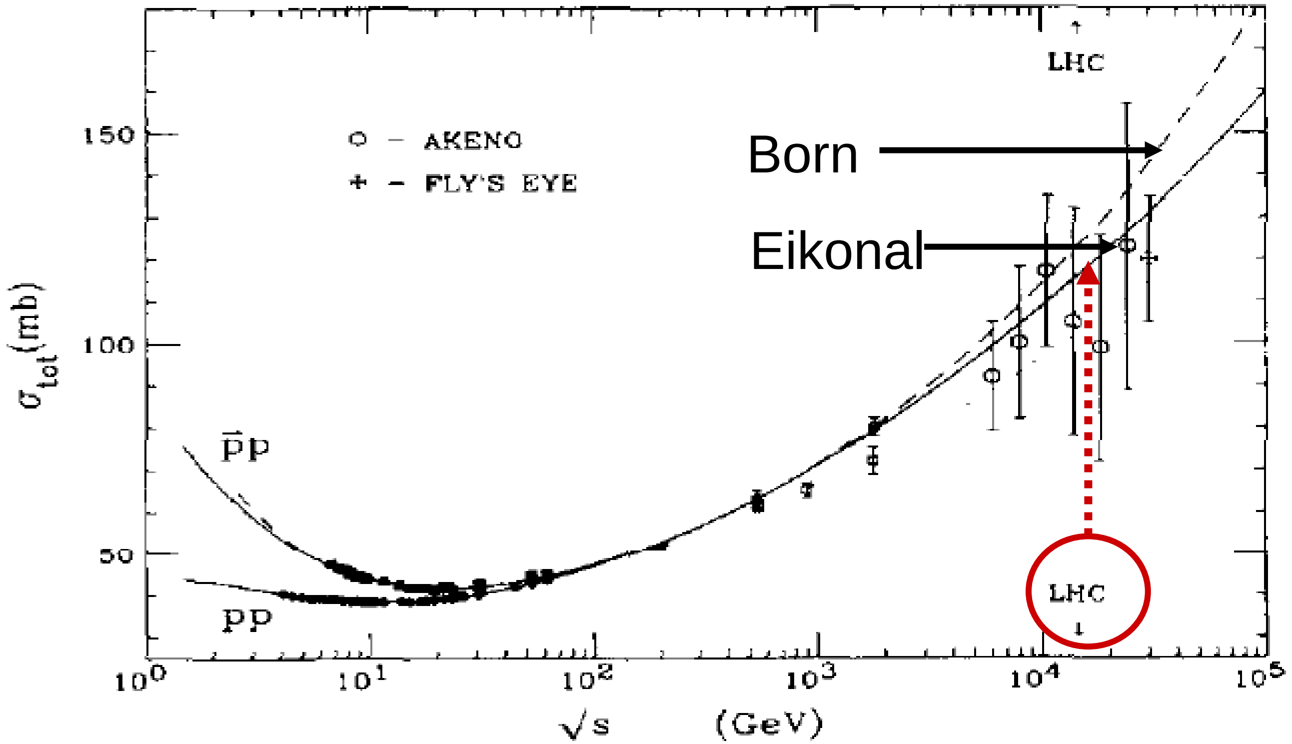

- σ @ LHC $\sqrt{s}$=14 TeV: 122 ± 5 mb Born, <u>114 ± 5 mb eikonal</u>
  ➔ error estimated from the error in ε given in CMG-96

Compare with **SUPERBALL** σ(14 TeV) = 113 ± 6 mb

caveat: s_o=1 GeV^2 was used in global fit!

Unitarity and Renormalization

Pomeron flux

s_0^{ε}

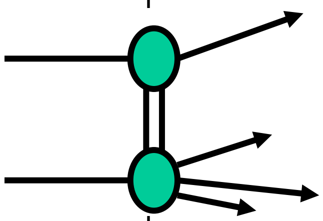

$$\frac{d^2\sigma_{SD}}{dt\,d\xi} = f_{IP/p}(t,\xi)\cdot\sigma_{IP-\bar{p}}(s\xi)$$

$s_0^{-\varepsilon/2}\cdot g_{PPP}(t)$

Pomeron-proton x-section

- Two free parameters: s_0 and g_{PPP}
- Obtain product $g_{PPP} \bullet s_0^{\varepsilon/2}$ from σ_{SD}
- Renormalized Pomeron flux determines s_0
- Get unique solution for g_{PPP}

The value of s_o - limited edition

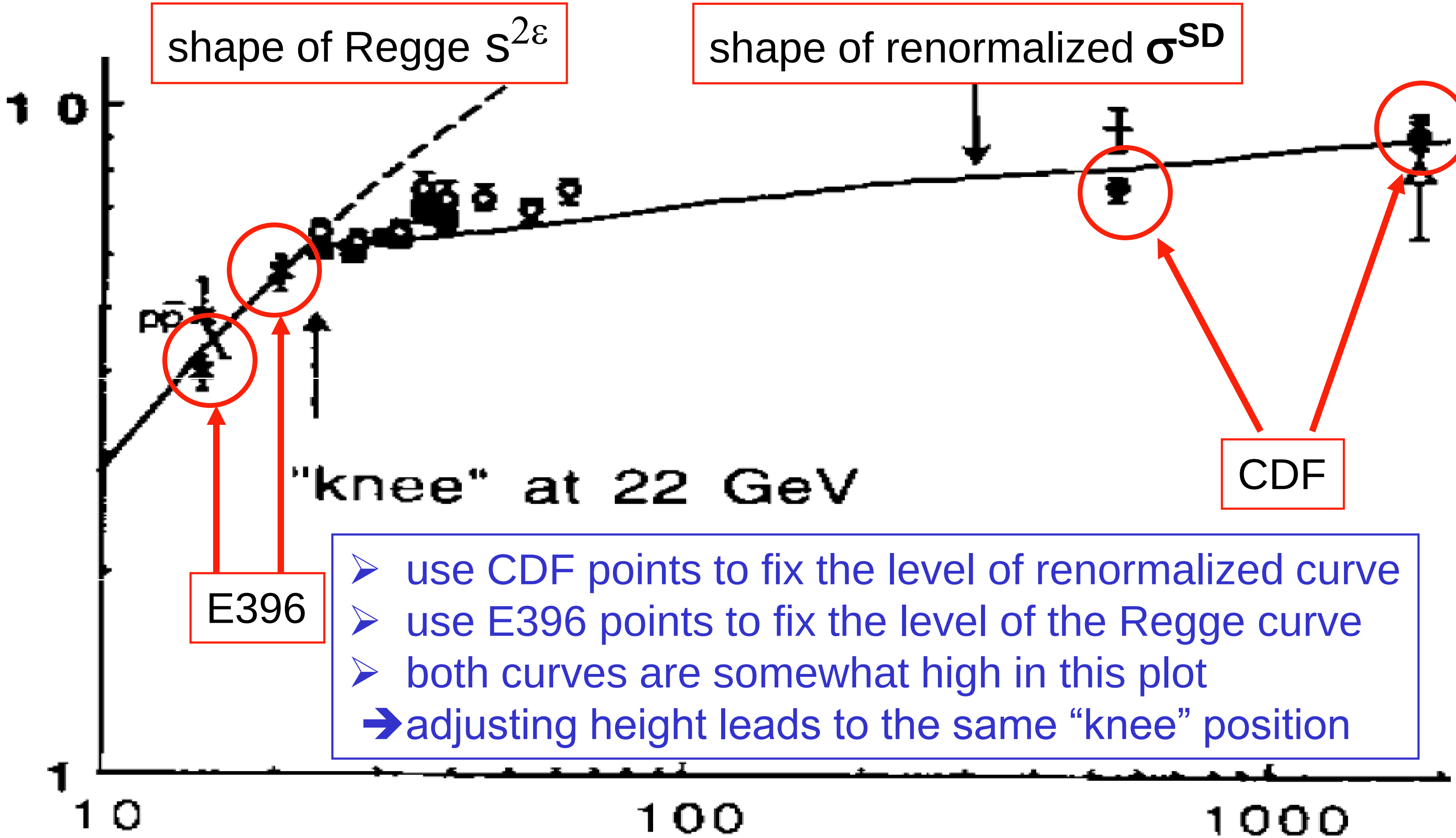

- use CDF points to fix the level of renormalized curve
- use E396 points to fix the level of the Regge curve
- both curves are somewhat high in this plot

➔adjusting height leads to the same "knee" position

The value of s_o - a bird's-eye view

KG-95

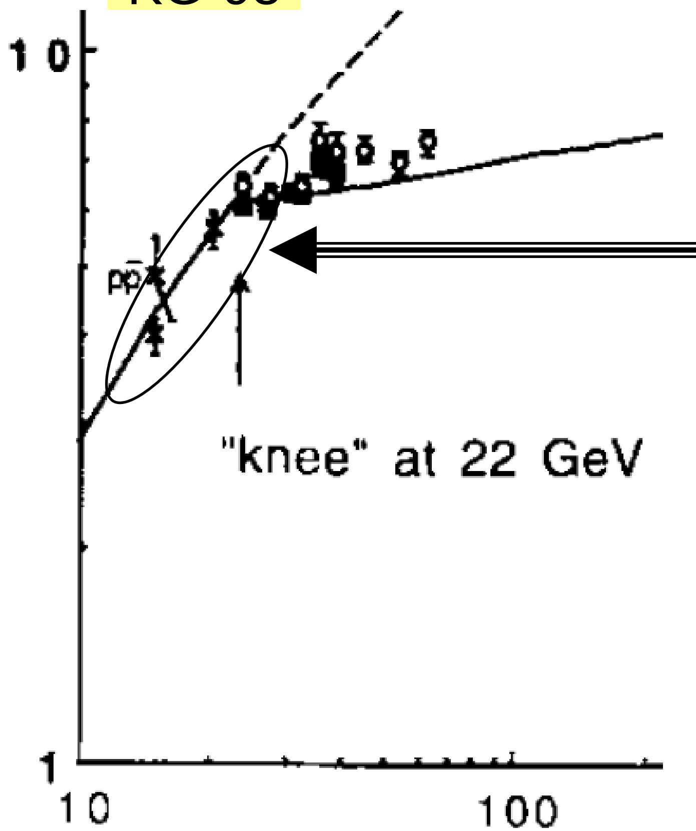

			$\sqrt{s}$ (GeV)	
⊠	Cool [KG]	FNAL	14	20
■	Albrow	ISR	23.3	26.9
o	Armitage	ISR	23.3	27.4

➔ error in knee position: ± 1 GeV

"knee" @ 22 ± 1 GeV ➔ $s_0 = 1 \pm 0.2$ GeV

➔riple-Pomeron coupling:

$$g_{PPP}(t) = 0.69\ \text{mb}^{1/2} = 1.1\ \text{GeV}^{-1}$$

KG-95

σ^T_{SD} and ratio of α'/ε

$$\frac{d^2\sigma(s,M^2,t)}{dM^2dt} = \left[\frac{\sigma_\circ}{16\pi}\sigma_\circ^{I\!Pp}\right]\frac{s^{2\epsilon}}{N(s)}\frac{1}{(M^2)^{1+\epsilon}}e^{bt}$$

$$\stackrel{s\to\infty}{\Rightarrow} \left[2\alpha' e^{\frac{\epsilon b_0}{\alpha'}}\sigma_\circ^{I\!Pp}\right]\frac{\ln s^{2\epsilon}}{(M^2)^{1+\epsilon}}e^{bt}, \quad (13)$$

$$\sigma_{sd} \stackrel{s\to\infty}{\rightarrow} 2\,\sigma_\circ^{I\!Pp}\ \exp\left[\frac{\epsilon b_0}{2\alpha'}\right] = \sigma_{sd}^\infty = \text{constant.} \quad (14)$$

$$2\sigma_\circ^{I\!Pp}\ \exp\left[\frac{\epsilon b_0}{2\alpha'}\right] = \sigma_0^{pp},$$

$$\sigma_\circ^{I\!Pp} = \beta_{I\!Ppp}(0)\cdot g(t) = \kappa\sigma_\circ^{pp}$$

$$\kappa = \frac{f_g^\infty}{N_c^2-1} + \frac{f_q^\infty}{N_c}$$

$$b_0 = R_p^2/2 = 1/(2m_\pi^2).$$

CTEQ5L→

$$f_g^\infty = 0.75$$

$$f_q^\infty = 0.25$$

$$r = \frac{\alpha'}{\epsilon} = -[16\,m_\pi^2\ln(2\kappa)]^{-1}$$

$$r_{pheno} = 3.2 \pm 0.4\ (\text{GeV/c})^{-2}$$

$$r_{exp} = 0.25\ (\text{GeV/c})^{-2}/0.08 = 3.13\ (\text{GeV/c})^{-2}$$

Total Cross Section at LHC

- Froissart bound $\sigma \leq \frac{\pi}{m^2} \cdot \ln^2 s$ (s in GeV^2)
- For $m^2 = m_\pi^2$ ➔ $\pi / m^2 \sim 10^4$ mb – large!
- If $m^2 = s_o$ = (mass)^2 of a large **SUPER**glue**BALL**, the bound can be reached at a much lower s-value, s_F,

➔ $\sigma(s > s_F) = \sigma(s_F) + \frac{\pi}{s_o} \cdot \ln^2 \frac{s}{s_F}$

- Determine s_F and s_0 from σ_T^{SD}
- Show that $\sqrt{s_F}$ < 1.8 TeV
- Show that at $\sqrt{s}$ = 1.8 TeV Reggeon contributions are negligible
- Get cross section at the LHC as

$$\sigma^{LHC} = \sigma_{1800}^{CDF} + \frac{\pi}{\mathbf{s_0}} \cdot \left(\ln^2 \frac{s^{LHC}}{s_F} - \ln^2 \frac{s^{CDF}}{s_F} \right)$$

The **SUPERBALL** cross-section

- Froissart bound $$\sigma \leq \frac{\pi}{m^2} \cdot \ln^2 s$$
- Valid above "knee" at √s = 22 GeV and therefore at √s = 1.8 TeV
- Use superball mass:

  ➔ $m^2 = s_0 = (1 \pm 0.2)\ \mathrm{GeV}^2$

- At √s 1.8 TeV Reggeon contributions are negligible (see global fit)

$$\sigma_{14000}^{LHC} = \sigma_{1800}^{CDF} + \frac{\pi}{s_0} \cdot \left(\ln^2 \frac{s^{LHC}}{s_F} - \ln^2 \frac{s^{CDF}}{s_F} \right) = (80.03 \pm 2.24) + (39 \pm 6) = 119 \pm 6 \text{ mb}$$

➔ compatible with CGM-96 global fit result of 114 ± 5 mb (see next slides)

The Roman-Pot Detectors at CDF

BACKUP

Concept of a Roman Pot

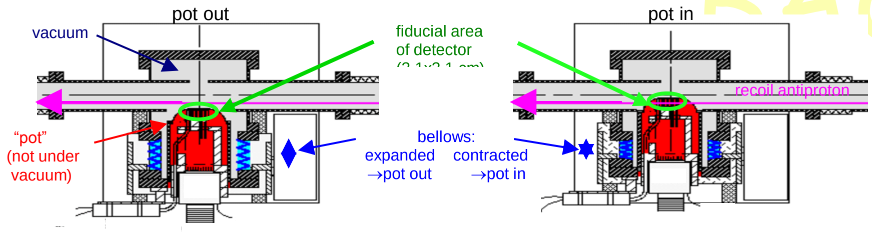

Bellows allow detectors to move close to the beam while maintaining vacuum

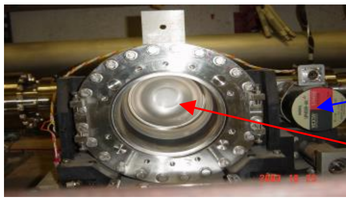

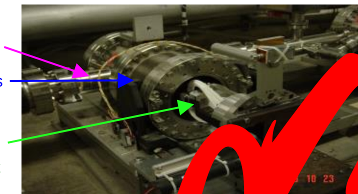

In the Tevatron Tunnel

CDF had three Roman pots (RP1, RP2, RP3) located 57m downstream of the interaction point along the antiproton beam direction. They were used to detect antiprotons which underwent a "diffractive" interaction and were scattered in a direction very close to that of the original beam.

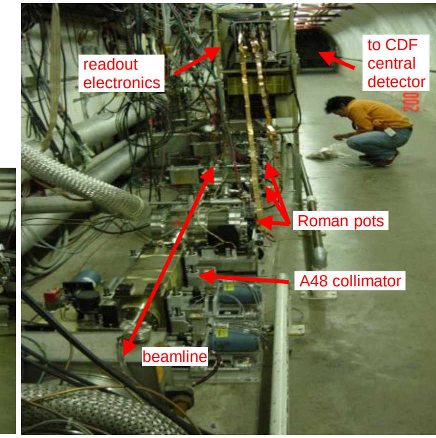

Roman-Pot Detector Design – by The Rockefeller University

The three Roman pots each contain detectors consisting of:

- Trigger scintillation counter 2.1x2.1x0.8 cm^3
- 40 X + 40 Y fiber readout channels
  - Each consists of 4 (→ bigger signal) clad scintillating fibers 0.8x0.8 mm^2 (new technology at the time)
  - X,Y each have 2 rows of 20 fibers spaced 1/3 fiber width apart for improved position resolution (three times better than with a single row)

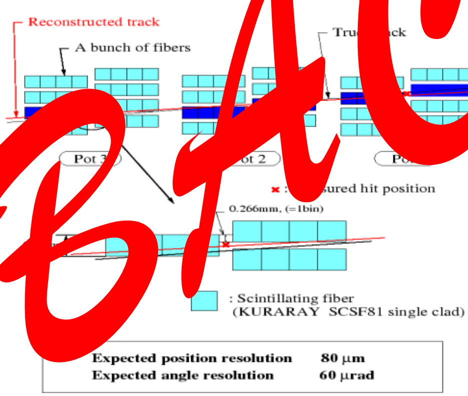

CDF "Tokyo"-Pot Detectors – Built by the University of Tsukuba, Japan

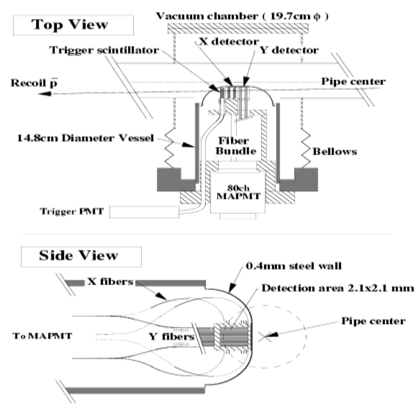

Physics Using the Roman-Pot Detectors

- The Roman-pot detectors are used to study diffractive interactions
- Elastic scattering was measured by CDF in 1988-1989 using Roman pots (not those described here) in both the proton and antiproton direction

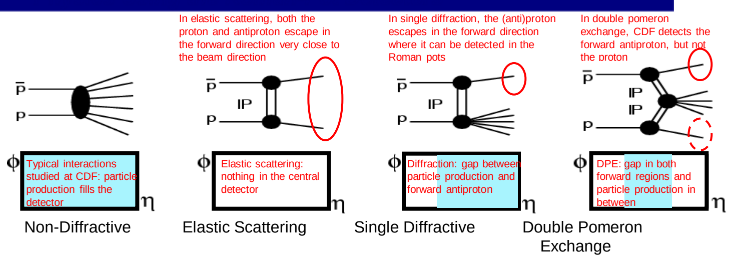

Path of the Antiproton through the Tevatron Magnets

- Dipole magnets bend recoil antiprotons which have lost momentum towards the inside of the Tevatron ring, into the Roman pots
- Knowledge of the beam optics, the collision vertex position, and the antiproton track position and angle in the Roman-pot detectors are used to reconstruct the kinematics of the diffractive antiproton

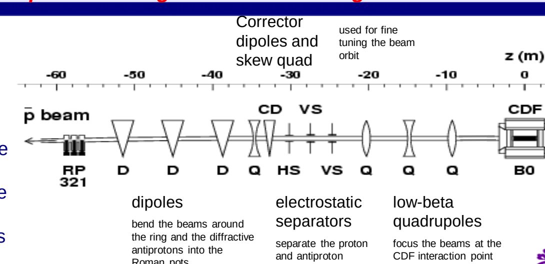

Gap survival probability

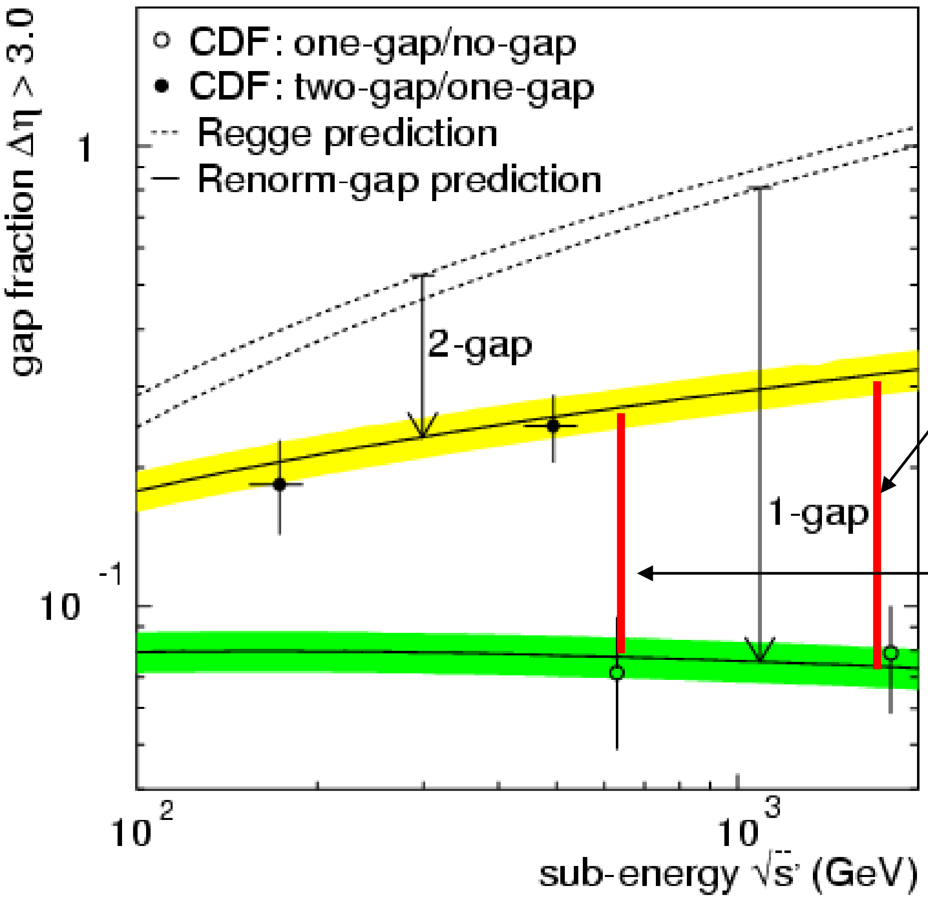

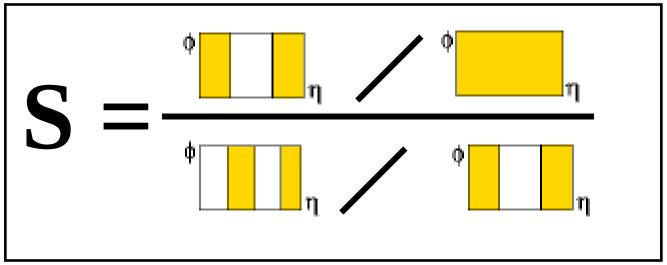

$$S^{1-gap/0-gap}_{2-gap/1-gap}(1800\ \mathrm{GeV}) \approx 0.23$$

$$S^{1-gap/0-gap}_{2-gap/1-gap}(630\ \mathrm{GeV}) \approx 0.29$$

CDF and D0 Detectors

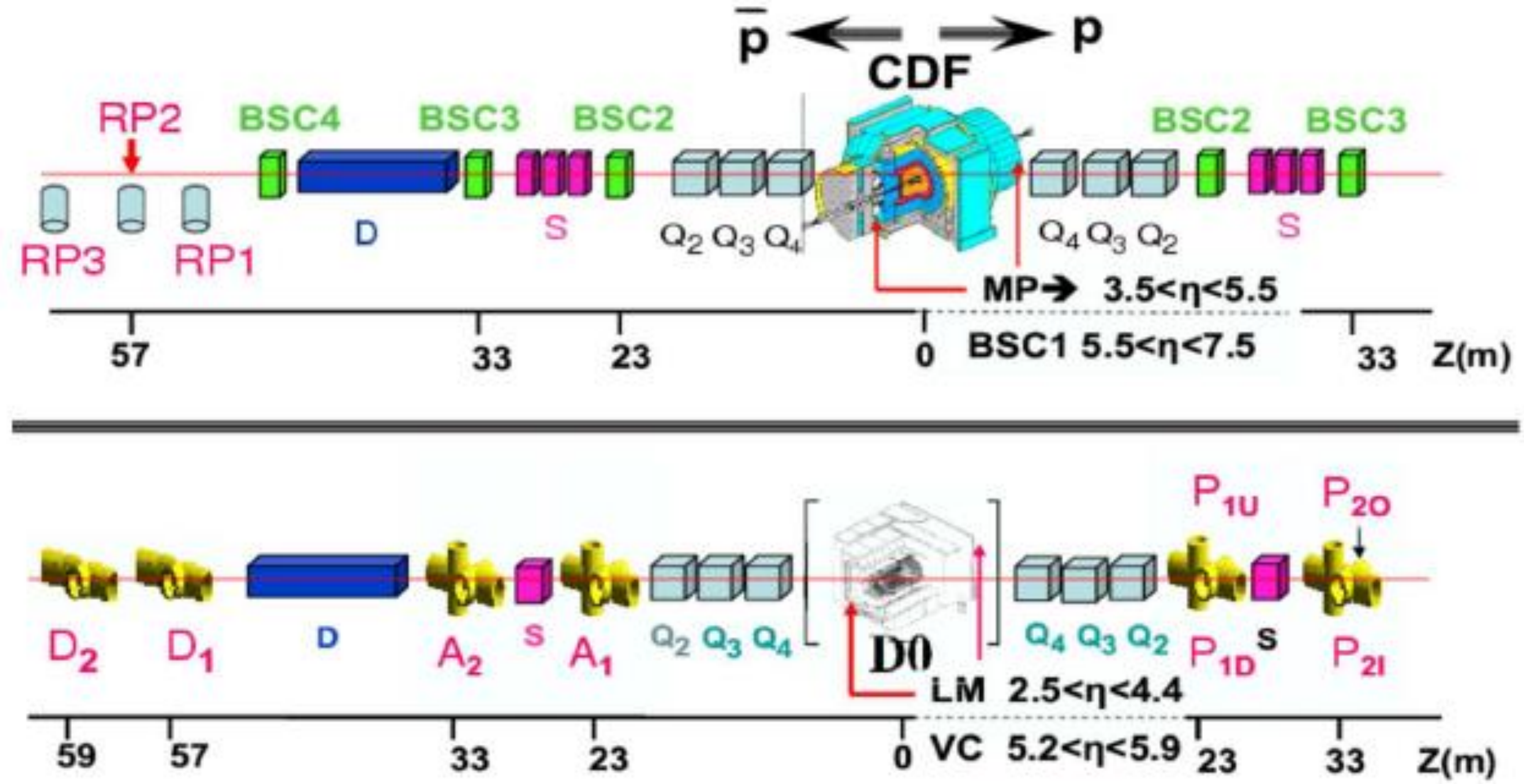

Figure 1: The CDF and D0 detectors in Run II